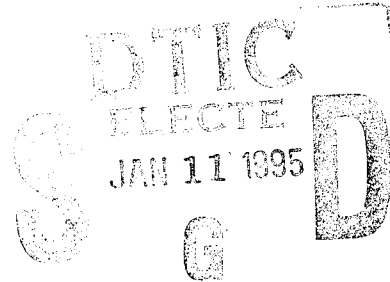# NATIONAL AIR INTELLIGENCE CENTER

A NUMERICAL METHOD FOR UNSTEADY TRANSONIC FLOW
ABOUT WINGS WITH CONTROL SURFACES

by

Yu Tao, Zhang Jianbai

DTIC
ELECTE
JAN 11 1995
G

19950109 118

| Accesion For | | |
|---|---|---|
| NTIS CRA&I | | ☒ |
| DTIC TAB | | ☐ |
| Unannounced | | ☐ |
| Justification | | |
| By | | |
| Distribution / | | |
| Availability Codes | | |
| Dist | Avail and / or Special | |
| A-1 | | |

# HUMAN TRANSLATION

NAIC-ID(RS)T-0920-92          15 December 1994

MICROFICHE NR: 94C000 557

A NUMERICAL METHOD FOR UNSTEADY TRANSONIC FLOW
ABOUT WINGS WITH CONTROL SURFACES

By: Yu Tao, Zhang Jianbai

English pages: 13

Source: Kongqidonglixue Xuebao, Vol. 9, Nr. 3, September
1991; pp. 338-343

Country of origin: China
Translated by: SCITRAN
          F33657-84-D-0165
Quality Control: Nancy L. Burns
Requester: NAIC/TATV/Paul F. Freisthler
Approved for public release; Distribution unlimited.

## GRAPHICS DISCLAIMER

All figures, graphics, tables, equations, etc. merged into this
translation were extracted from the best quality copy available.

# A NUMERICAL METHOD FOR UNSTEADY TRANSONIC FLOW
## ABOUT WINGS WITH CONTROL SURFACES

Yu Tao   Zhang Jianbai

## ABSTRACT

This article introduces a type of finite difference calculation method for unsteady transonic speed flows associated with wings having control surfaces. The equations which are chosen for use are modified three dimensional nonsteady transonic speed small perturbation geopotential equations. Use is made of time integration methods. Solution forms are approximate factor type resolutions of alternating direction implicit (ADI) type forms. Use is made of this type of method to calculate the unsteady aerodynamic forces associated with F-5 wings in oncoming flows with Mach numbers or 0.9 and 0.925 as well as the unsteady aerodynamic forces associated with control surface oscillations. Comparisons were carried out of calculation results with NLR test results from outside of China and calculation results from XTRAN3S methods. This clearly showed that calculations were successful.

## INTRODUCTION

As is known by everyone, the transonic speed range is the zone in which the occurrence of aircraft wing vibration phenomena is most severe and most dangerous. Due to actual aircraft wings all having control surfaces, making use of control surface oscillations to restrain vibration is a hot topic at the present time. There is a need to study the influences of control surface oscillations on wing vibrations. It is then necessary to have accurate numerical value calculation methods for unsteady transonic winding flows associated with wings having control surfaces.

---

* Numbers in margins indicate foreign pagination.
Commas in numbers indicate decimals.

The China Aerodynamics Research and Development Center has already test produced a three dimensional unsteady transonic flow numerical value calculation method--the CTRAN3S program. The equations solved are three dimensional unsteady transonic flow modified small perturbation geopotential equations. The solution forms are approximate factor type resolution alternating direction implicit type (ADI) difference forms. Use is made of time integration methods. It accurately handles equation nonlinearity, figuring in shock wave movements on wing surfaces. See also Refernces [1-4].

This article is based on the foundation of CTRAN3S methods. It calculates unsteady transonic aerodynamic forces associated with wings having control surfaces and expands the functions of the CTRAN3S program in calculating nonsteady aerodynamic forces.

This article calculates, for the two states with oncoming flow Mach numbers of 0.9 and 0.925, the steady state and non-steady state transonic aerodynamic forces associated with F-5 wings having inboard trailing edge control surfaces. The results from this article are compared relative to NLR test results from outside China as well as calculation results from XTRAN3S methods. The consistency is very good. In order to study a step further the analyzing of transonic nonlinear vibration in wings having control surfaces and the restraining of the motive forces of vibration, it provides effective analytical tools.


I. BASIC EQUATTIONS AND BOUNDARY CONDITIONS


Given geopotential assumptions, the conservation forms associated with modified small perturbation geopotential equations for three dimensional non-steady state transonic flows are capable of being written as

2

$$-\frac{\partial f_0}{\partial t}+\frac{\partial f_1}{\partial x}+\frac{\partial f_2}{\partial y}+\frac{\partial f_3}{\partial z}=0 \qquad (1)$$

In this

$$f_0 = A\,\phi_t + B\,\phi_x \qquad (2a)$$

$$f_1 = E\,\phi_x + F\,\phi_x^2 + G\,\phi_y^2 \qquad (2b)$$

$$f_2 = \phi_y + H\,\phi_x\,\phi_y \qquad (2c)$$

$$f_3 = \phi_z \qquad (2d)$$

Here $\phi$ is a small perturbation geopotential. The subscripts x, y, and z are derivatives expressing the directions in question. Moreover,

$$A = k^2 M^2 \qquad (3a)$$

$$B = 2k M^2 \qquad (3b)$$

$$E = 1 - M^2 \qquad (3c)$$

As far as the spacial coordinates x, y, and z are concerned, use is already made of wing base or tab chord length c for nondimensional transition. With regard to time t, use is already made of the inverse $1/\omega$ associated with oscillation frequency for nondimensional transition. In the case of $\phi$, use is already made of the product of oncoming flow speed and wing base or tab chord lenth Uc in order to make a nondimensional transition. M is the Mach number of the oncoming flow. $k = \omega c/U$ is the reduction frequency. In order to accurately capture shock waves, as far as the nonlinearity coefficients are concerned, option was made for the use of NASA Ames coefficients

$$F = -(1/2)(\gamma+1)M^2 \qquad (4a)$$

$$G = (1/2)(\gamma-3)M^2 \qquad (4b)$$

$$H = -(\gamma-1)M^2 \qquad (4c)$$

Distant field boundary conditions for flow movements are

$$\phi = 0 \qquad \text{(far up stream)} \quad (5a)$$

$$\phi_x + k\phi_t = 0 \qquad \text{(far down stream)} \quad (5b)$$

3

$$\phi_z = 0 \qquad \text{(far upper and lower areas) (5c)}$$
$$\phi_y = 0 \qquad \text{(far direction of development) (5d)}$$
$$\phi_y = 0 \qquad \text{(wing root or tab symmetry conditions) (5e)}$$

Wing surfaces are defined as $\qquad z = f^{\pm}(x, y, t)$

The linearizing non-steady state boundary conditions are

$$\phi_z^{\pm} = f_x^{\pm} + k f_t^{\pm}$$

This is appropriate for use when $\quad z = 0^{\pm}, \ x_{le} \leq x \leq x_{te}, \ y \leq y_{tip}$

In the equations, the suprescript "$\pm$" represents upper and lower surfaces. The subscripts le and te represent leading edge and trailing edge; tip represents the wing tip.

Wake vortex conditions, when z = 0 and x > $x_{te}$, are defined as

$$\Delta \phi_z = 0 \qquad \text{(slope continuity)} \qquad \text{(6a)}$$
$$\Delta \phi_x + \Delta k \phi_t = 0 \quad \text{(pressure continuity) (6b)}$$

Before solving non-steady state problems, one first makes k = 0. Use is made of steady state boundary conditions to solve the equations discussed above. Using stability methods, one obtains the initial steady state solution

$$\phi(x, y, z, 0) = g(x, y, z) \qquad \text{(7a)}$$
$$\phi_t(x, y, z, 0) = 0 \qquad\qquad \text{(7b)}$$

Subsequent to that, one takes k values associated with the actual conditions and substitutes them into equations and boundary conditions, solving again. It is then possible to make fully precise determinations for non-steady state problems.

As far as the boundary conditions for wings having control surfaces are concerned, besides the differences between the linearized non-steady state boundary conditions and wings having

4

control surfaces, their distant field and wake vortex conditions
are all the same as the initial conditions. Assuming $z = f_A^{\pm}(x, y, z, t)$
represents the instantaneous surface configurations associated
with wings having control surfaces. The linearized non-steady
state boundary conditions are

$$\phi_z^{\pm} = f_{Ax}^{\pm} + k f_{At}^{\pm} \qquad (8)$$

This is appropriate for use with $z = 0^{\pm}$, $x_{hl} < x \leq x_{le}$, $y_a \leq y \leq y_b$

In the equation, xhl represents the location of the hinge lines
of control surfaces. ya and yb, respectively, represent
deployment direction locations for the two sides of control
surfaces. $f_A^{\pm}(x, y, z, t)$ is capable of being divided into
steady state portions (wing surface geometrical configurations
and angles of attack) and non-steady state portions (vibration
forms). The steady state portions of it and the steady state
portions associated with wings not having control surfaces are
the same. Non-steady state portions are different. Actual lower
flow conditions are

$$\phi_z^{\pm} = (\partial f_A^{\pm} / \partial x)_s + (\partial f_A^{\pm} / \partial x)_{us} + k(\partial f_A^{\pm} / \partial t)_{us} \qquad (9)$$

In the equations, the subscript s stands for steady, us
indicates unsteady. Assume a is the wing angle of attack. $\delta$ is
the control surface oscillation amplitude angle or argument.
[ $[\begin{smallmatrix}0\\1\end{smallmatrix}]_l$ ] stands for choosing 1 on control surfaces and 0 off control
surfaces. Then, one has

$$(\partial f_A^{\pm} / \partial x)_{us} = -\{\delta \cdot \sin(kt)\}[\begin{smallmatrix}0\\1\end{smallmatrix}]_l \qquad (10a)$$
$$k(\partial f_A^{\pm} / \partial t)_{us} = -\{k \cdot \delta(x - x_{hl}) \cdot \cos(kt)\}[\begin{smallmatrix}0\\1\end{smallmatrix}]_l \qquad (10b)$$

In this way, one then obtains a method to calculate unsteady
transonic gas flow forces on wings having control surfaces. We
are constrained by the scope of this article. As far as the

5

method's details and coordinate transformations, and so on, are concerned, please see References [1-4].


## II.  CALCULATION RESULTS AND DISCUSSION

This article calculates steady and unsteady gas dynamics associated with F-5 wings having control surfaces. The incoming flow Mach numbers for the calculations are 0.9 and 0.925. The reductions frequency k is equal to 0.137. The angle of amplitude or argument δ associated with control surface oscillations is 0.5°. The frequency is 20 Hz. The grid point numbers are 47x15x28 (chord x span x normal direction).
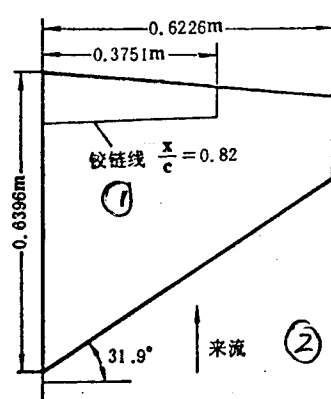


Fig.1 The F-5 Wing Platform with Trailing Edge Flap

Key: (1)  Hinge Line  (2)  Incoming Flow


Fig.1 is aschematic diagram of an F-5 wing having control surfaces. The F-5 wing is a triangular wing with the tip cut off and a small span-chord ratio. The span-chord ratio is 2.98. The taper ratio is 0.31. The angle of backward sweep on the leading edge is 31.92°. The form of the wing cross section is a revised NACA 65-A-0048 wing form. The head section hangs down to 40% chord length. After 40% chord length, the wing form is

symmetrical. The calculated control surface hinge line is located at the x/c = 0.82 position. The span direction runs from the wing root or tab to $\eta$ = 0.5864. In the calculations, it is assumed that the wings and the control surfaces are all rigid surfaces.

Unsteady pressure calculation formulas are as shown below (see Reference [3])

$$C_{p_r} = [C_p(\omega t = \pi/2) - C_p(\omega t = 3\pi/2)]/(2\Delta\alpha) \qquad (11a)$$
$$C_{p_i} = [C_p(\omega t = 0) - C_p(\omega t = \pi)]/(2\Delta\alpha) \qquad (11b)$$

In the formulas, the subscript i stands for imaginary parts. r stands for real parts. $\Delta\alpha$ is taken as $\delta$, $C_p$. $C_p$ is selected for use as the values corresponding to the second period.

Fig.2 is a steady pressure distribution comparison figure associated with a 78% cross section when M = 0.9. In the Fig., NLR experimental data and XTRAN3S calculated data are both quoted from Reference [5]. When calculations are used, the increment length is $\Delta t$ = 0.037. 1000 increments were calculated. However, using XTRAN3S calculations, $\Delta t$ = 0.01. 4000 increments are calculated. From Fig.2, it is possible to know that the match up of calculation results between the calculated pressure distributions in question and the NLR experimental results as well as the calculation results associated with XTRAN3S is very good.

/341

Fig. 3 is a surface unsteady pressure distribution comparison figure on a 19% cross section. Fig.4 is a comparison figure associated with a 79% cross section. The calculations in question use $\Delta t$ = 0.0425. Each period calculates 540 increments. 1 3/4 periods are calculated. There is a total calculation of 945 increments. XTRAN3S calculations opt for the use of $\Delta t$ = 0.01102. Each period figures 2160 increments.

7

3 periods were calculated.  There were a total of 6480 increments calculated.  See Reference [5].  From Fig.3 and Fig.4, one knows that the real parts of peak values for unsteady pressures on surfaces in the calculations in question are somewhat lower than the XTRAN3S calculation results.  The imaginary parts, by contrast, are somewhat higher.  However, the results in question approach NLR experimental results even more closely than do XTRAN3S calculation results.  The shock wave locations obtained from these calculations and experimental results are almost completely identical.  Pressure distribution results on control surfaces are also in mutual agreement.
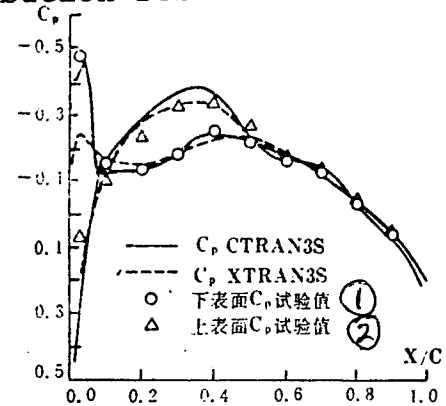
Fig.2   Comparison of Steady Pressures, Theory and Experiment
M=0.9    a = o°, η = 78% Semispan

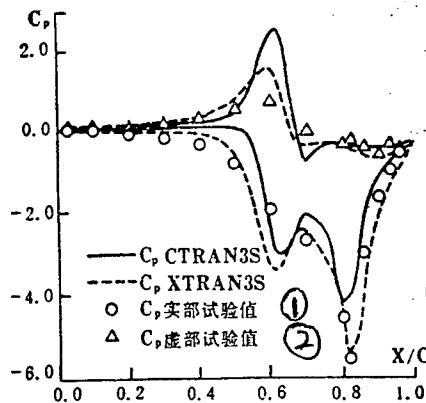Key: (1)   Lower Surface Cp Test Value (2)   Upper Surface Cp Test Value

Fig.3   Unsteady Upper Surface Pressure Comparison at M = 0.9, a = 0°, ,δ= ·0.5°,η=19%        Semispan

Key: (1) Cp Real Part Experimental Value   (2)   Cp Imaginary Part Experimental Value

8

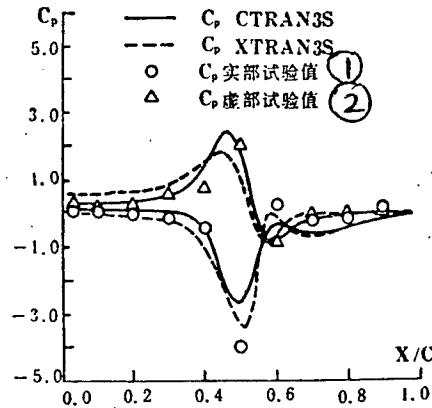Fig.5 is a steady pressure distribution comparison figure for a 78% cross section when M = 0.925.



Fig.4  Unsteady Upper Surface Pressure Comparison at M = 0.9, $\alpha = 0°$, $\delta = 0.5°$, 79% semispan

Key: (1)  Cp Real Part Experimental Value  (2)  Cp Imaginary Part Experimental Value

The calculations in question make use of $\Delta t = 0.037$.  On the basis of a steady state associated with M = 0.9, they obtain additional calculations for 600 increments.  There are relative comparisons with NLR experimental results and XTRAN3S calculated results.  Shock wave positions are somewhat toward the rear. Shock waves are somewhat strong.  For XTRAN3S calculations, $\Delta t = 0.01$ with 3000 increments of iterative substitution.

9
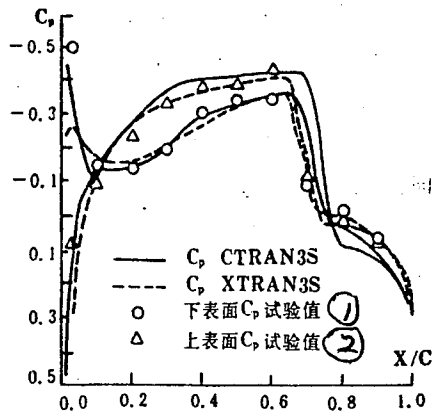
**Fig.5  Comparison of Steady Pressures, Theory and Experiment**
$M = 0.925, a = 0°, 78\%$ semispan

Key: (1)  Lower Surface Cp Experimental Values  (2) Upper Surface Cp Experimental Values

Fig.6 and Fig.7, respectively, are comparative figures for distributions of the real portions of upper surface unsteady pressures associated with 19% and 78% cross sections when M = 0.925.



**Fig.6  Unsteady Upper Surface Real Pressures Comparison at**
$M = 0.925, a = 0°, \delta = 0.5°, 19\%$ semispan

Key: (1)  Cp Real Part Experimental Value

**Fig.7 Unsteady Upper Surface Real Pressures Comparison at**
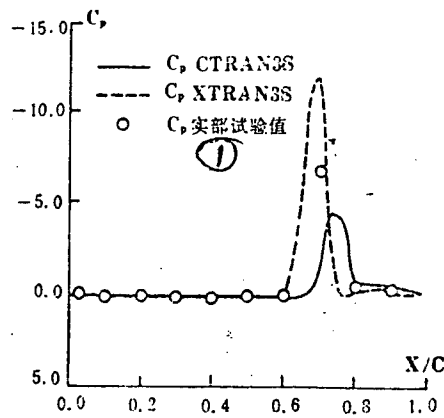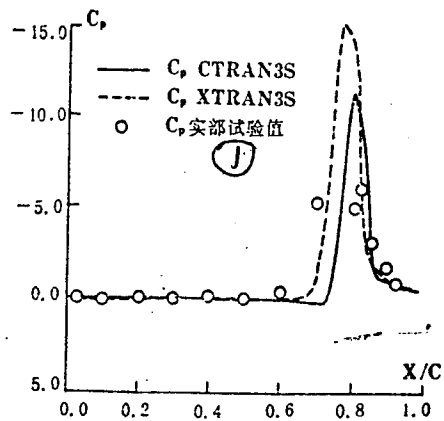$M = 0.925, \alpha = 0^\circ, \delta = 0.5^\circ, 78\%$ semispan

Key: (1) Cp Real Part Experimental Value


The calculations in question make use of $\Delta t = 0.0425$.
Each period calculates 540 increments. 1 3/4 periods were
calculated. There was a total calculation of 945 increments.
NLR experimental results and XTRAN3S calculation results were all
quoted from Reference [6]. The results in question were compared
with XTRAN3S calculation results and NLR experimental results.
The shock waves which were calculated out tended toward the rear
approximately 5%. Shock wave strengths were greater than NLR
experimental results. However, they were weaker than shock waves
calculated out by XTRAN3S.


Summing it all up, when M = 0.9, the results of the
calculations in question were compared to NLR experimental
results and XTRAN3S calculated results. Steady and unsteady
shock wave positions were all in almost complete accord with one

11

another.  Pressure distributions on control surfaces also matched up with each other.  When M = 0.925, shock wave positions for the calculations in question tended toward the rear 5%.  Compared to NLR experimental results, shock waves were relatively strong.  At this time, following along with increases in incoming flow Mach numbers, shock wave positions moved rearward.  Close to the forward edges of control surfaces, shock waves turned strong.  This is reasonable.  The calculations in question did not take into consideration the influences of viscosity.  If one carries corrections for viscosity a step further in the considerations, then, the calculations results for times when M = 0.925 and experimental results will agree even better.


## III.  CONCLUSIONS


On the basis of the preceeding analysis and discussion of calculation results, it is possible to come to the following conclusions.  Making use of the methods in question to calculate unsteady transonic aerodynamic problems for wings having control surfaces is successful.  As far as comparisons between the calculation results in question and XTRAN3S calculation results from outside China as well as NLR experimental results are concerned, the match up is quite good.  Due to the fact that the methods in question make use of grid point numbers which are 47x15x28, and each period of calculation increments is 540, while XTRAN3S calculations use grid point numbers which are 60x20x40 with each period of calculations as 2160 increments, this article, as a result of this, reduced very greatly the amount of calculations.  Calculation efficiency was very high.  Besides this, the applicability of the methods in question is relatively broad.  In principle, it is possible to calculate control surface wings at any position, for example, midspan, outside edge, and even down to forward edge control surfaces.  This will then supply a type of precision analytical tool for the study of

12

nonlinear transonic vibration as well as for restraining the driving forces of vibration.

## REFERENCES

[1]  Zhang Jianbai, "Three Dimensional Transonic Flow Numerical Value Solution Methods".  "China Aeronautical Technology Reference" HJB 8601410, (1986).

[2]  Zhang, J.B., AIAA 88-4352, (1988).

[3]  Zhang Jianbai, Aerodynamics Journal, 6, 4 (1988)

[4]  Zhang Jianbai, "Transonic Unsteady Aerodynamic Numerical Value Solution Methods for Rear Swept Fighter Type Wings", "China Aeronautic Technology Reference", HJB 890688, (1989)

[5]  Sotomayer, W.A., Borland, C.J., AIAA 85-1712.

[6]  Guruswamy, P.G., Coorjian, P.M., Tu. E.L., AIAA 87-0709.

```
                    DISTRIBUTION LIST
                    ------------------


               DISTRIBUTION DIRECT TO RECIPIENT
               -------------------------------------


     ORGANIZATION                            MICROFICHE
     ------------                            ----------


     B085 DIA/RTS-2FI                            1
     C509 BALL0C509 BALLISTIC RES LAB            1
     C510 R&T LABS/AVEADCOM                      1
     C513 ARRADCOM                               1
     C535 AVRADCOM/TSARCOM                       1
     C539 TRASANA                                1
     Q592 FSTC                                   4
     Q619 MSIC REDSTONE                          1
     Q008 NTIC                                   1
     Q043 AFMIC-IS                               1
     E051 HQ USAF/INET                           1
     E404 AEDC/DOF                               1
     E408 AFWL                                   1
     E410 AFDTC/IN                               1
     E429 SD/IND                                 1
     P005 DOE/ISA/DDI                            1
     P050 CIA/OCR/ADD/SD                         2
     1051 AFIT/LDE                               1
     P090 NSA/CDB                                1
     2206 FSL                                    1
```

Microfiche Nbr: FTD94C000557
NAIC-ID(RS)T-0920-92